Journal of Neurochemistry

JOURNAL OF NEUROCHEMISTRY | 2009 | 110 | 1818–1827 doi: 10.1111/j.1471-4159.2009.06277.x

Age-dependent dysregulation of brain amyloid precursor protein in the Ts65Dn Down syndrome mouse model

Jennifer H. K. Choi,*,† Jason D. Berger,* Matthew J. Mazzella,* Jose Morales-Corraliza,*,‡ Anne M. Cataldo,§,¶,** Ralph A. Nixon,*,‡,‡‡ Stephen D. Ginsberg,*,†,‡ Efrat Levy*,‡,†† and Paul M. Mathews*,‡

*Center for Dementia Research, Nathan Kline Institute, Orangeburg, New York, USA

Departments of †Physiology & Neuroscience, ‡Psychiatry, ††Pharmacology and ‡‡Cell Biology, NYU School of Medicine, New York, New York, USA

§Laboratory of Molecular Neuropathology, Mailman Research Center, McLean Hospital, Belmont, Massachusets, USA

Departments of ¶Psychiatry and **Neuropathology, Harvard Medical School, Boston, Massachusets, USA

Abstract

Individuals with Down syndrome develop β-amyloid deposition characteristic of early-onset Alzheimer's disease (AD) in mid-life, presumably because of an extra copy of the chromosome 21-located amyloid precursor protein (*App*) gene. *App* mRNA and APP metabolite levels were assessed in the brains of Ts65Dn mice, a mouse model of Down syndrome, using quantitative PCR, western blot analysis, immunoprecipitation, and ELISAs. In spite of the additional *App* gene copy, *App* mRNA, APP holoprotein, and all APP metabolite levels in the brains of 4-month-old trisomic mice were not increased compared with the levels seen in diploid littermate controls. However starting at 10 months of age, brain APP levels were increased proportional to the *App* gene dosage imbalance reflecting increased *App* message levels in Ts65Dn mice. Similar to APP levels, soluble amino-terminal fragments of APP (sAPPα and sAPPβ) were increased in Ts65Dn mice compared with diploid mice at 12 months but not at 4 months of age. Brain levels of both Aβ40 and Aβ42 were not increased in Ts65Dn mice compared with diploid mice at all ages examined. Therefore, multiple mechanisms contribute to the regulation towards diploid levels of APP metabolites in the Ts65Dn mouse brain.

Keywords: Alzheimer's disease, amyloid precursor protein, animal model, Down syndrome, trisomy.

J. Neurochem. (2009) **110**, 1818–1827.

In mid-life, Down syndrome (DS) or trisomy 21 individuals develop early-onset Alzheimer's disease (AD)-like dementia and age-related AD pathologies (Casanova *et al.* 1985; Mann *et al.* 1989), including deposition of the amyloid β peptide (Aβ) as insoluble β-amyloid plaques in the brain parenchyma and around the cerebrovasculature (Hardy and Selkoe 2002). As the amyloid precursor protein (*App*) gene is located on human chromosome 21 (HSA21), *App* triplication is thought to contribute to the early-onset AD phenotype in DS patients. Analyses of families with small duplications of a very small region containing the *App* gene on HSA21 support the view that *App* triplication alone is sufficient to cause AD pathology in humans (Rovelet-Lecrux *et al.* 2006; Sleegers *et al.* 2006). While this finding implicates *App* gene dosage in the eventual development of AD pathology in DS patients, the relationship between *App* gene copy levels, APP protein levels, and DS neuropathology – including, but not limited to β-amyloidosis – is age-dependent and is likely to be multifactorial.

A widely used experimental mouse model of human DS is the Ts65Dn mouse, which is trisomic for a segment of murine chromosome 16 orthologous to the DS critical region

Received March 26, 2009; revised manuscript received July 2, 2009; accepted July 3, 2009.

Address correspondence and reprint requests to Jennifer Choi or Paul Mathews, Ph.D., New York University School of Medicine, Nathan Kline Institute, 140 Old Orangeburg Rd., Orangeburg, NY 10962, USA. E-mail: jchoi@nki.rfmh.org or mathews@nki.rfmh.org

Abbreviations used: Aβ, amyloid β peptide; AD, Alzheimer's disease; APP, amyloid precursor protein; BFCN, basal forebrain cholinergic neuron; CTF, C-terminal fragment; DS, Down syndrome; IDE, insulin degrading enzyme; NGF, nerve growth factor; qPCR, quantitative PCR; sAPP, soluble amino-terminal fragment of APP; SOD1, superoxide dismutase.

of HSA21, which includes the *App* gene (Reeves *et al.* 1995). Ts65Dn mice exhibit developmental delay (Holtzman *et al.* 1996) and abnormal behaviors (Reeves *et al.* 1995) that appear to be analogous to mental retardation in DS patients. These learning deficits correlate with age-related neuronal atrophy, neurodegenerative changes, and loss of nerve growth factor (NGF) retrograde transport that results in the degeneration of basal forebrain cholinergic neurons (BFCNs) (Cooper *et al.* 2001; Granholm *et al.* 2003; Salehi *et al.* 2006). Similar to human DS, the Ts65Dn mouse also develops AD-like neuronal endosomal pathology (Cataldo *et al.* 2003), pathological changes which are likely to underlie the failure of NGF-mediated trophic support in this model through signaling endosomes (Wu *et al.* 2009).

Crossing the Ts65Dn mouse with a mouse carrying an APP null allele to restore *App* gene copy to 2N levels has shown that triplication of the *App* gene is necessary for the development of the abnormally large neuronal endosomes (Cataldo *et al.* 2003) and for the defective retrograde NGF trophic support seen in the Ts65Dn mouse (Salehi *et al.* 2006). While reduction of *App* gene dosage to 2N levels in Ts65Dn mice reduces neuronal endosomal pathology and BFCN degeneration, the interpretation of these genetic experiments is complex given the proteolytic processing of APP into multiple, and potentially both neurotrophic and neurotoxic metabolites. Proteolytic processing of APP by both α- and β-cleavage generates soluble amino-terminal fragments of APP (sAPPα and sAPPβ), which are abundant in the brain and have been shown to have neurotrophic effects *in vitro* in conjunction with NGF (Wallace *et al.* 1997; Wang *et al.* 2000). In contrast to the neurotrophic sAPP fragments, β-cleavage followed by γ-cleavage yields various Aβ peptides, which have been shown to have neurotoxic effects in multiple experimental systems (Lin *et al.* 2000; Hardy and Selkoe 2002; Vetrivel and Thinakaran 2006). Because the Ts65Dn mouse has age-related decreased cognitive ability (Reeves *et al.* 1995; Demas *et al.* 1996, 1998; Holtzman *et al.* 1996; Hunter *et al.* 2003a) and *App*-gene dosage-dependent loss of vulnerable BFCNs (Granholm *et al.* 2000; Cooper *et al.* 2001), it is a good model system to examine *in vivo* the potential interplay between *App* gene triplication, aging, neurodegeneration, and APP proteolysis and metabolism.

Materials and methods

Mice and cycloheximide treatment

All mouse experimentation and animal care was approved by the Nathan S. Kline Institute's Institutional Animal Care and Use Committee. Ts65Dn mice ($n = 37$) were maintained on a mixed background (C57BL/6jEi × C3H/HeSnJ) and 2N littermates ($n = 42$) were used as control animals. APP null mice were purchased from Jackson Laboratory Mice and Services (Bar Harbor, ME, USA). Mice were killed and brains were immediately dissected and frozen on dry ice. For protein-based analyses, frozen hemibrains were homogenized as previously described with protease inhibitors (Schmidt *et al.* 2005b). For quantitative PCR (qPCR), frozen cortex was extracted in TRIzol LS Reagent (Gibco/Invitrogen, Carlsbad, CA, USA) prior to RNA isolation as per the manufacturer's instructions. To block protein synthesis in the brain, a cohort of Ts65Dn mice and their control 2N littermates were injected intraperitoneally with 100 μL of 150 μg/mL cycloheximide prepared in pH-buffered saline (Gold and Sternberg 1978), and killed post-injection as indicated prior to brain dissection (Morales-Corraliza J., Mazzella M.J., Berger J.D., Diaz N.S., Choi J.H.K., Levy E., Matsuoka Y., Planel E., and Mathews P.M., unpublished data).

Antibodies

The anti-APP C-terminal monoclonal antibody C1/6.1 recognizes both mouse and human APP holoprotein and C-terminal fragments (CTFs) (Mathews *et al.* 2002). The monoclonal m3.2 antibody is murine-specific and recognizes APP holoprotein, sAPPα, βCTF, and Aβ. In combination with Aβ40 and Aβ42 C-terminal specific monoclonal antibodies (JRF/cAβ40/10 and JRF/cAβ42/26), m3.2 was used as previously described to detect endogenous murine Aβ in Aβ40- and Aβ42-specific sandwich ELISAs (Schmidt *et al.* 2005a). To detect both species of sAPP, 22C11 (Millipore, Temecula, CA, USA) was used. Neprilysin (EC 3.4.24.11) was detected with the monoclonal antibody 56C6 (CD10) (Novacastra, Newcastle, UK), and insulin degrading enzyme (gift from Dr. Dennis Selkoe, Harvard Medical School, Boston, MA, USA) (IDE, EC 3.4.24.56) with the rabbit polyclonal antibody anti-IDE1 (Qiu *et al.* 1998). Superoxide dismutase (SOD1, EC 1.15.1.1) was detected with a rabbit polyclonal antibody anti-SOD1 (FL-154; Santa Cruz Biotechnology, Santa Cruz, CA, USA).

Biochemistry and ELISA

For western blot analysis, proteins were separated by sodium dodecyl sulfate–polyacrylamide gel electrophoresis and transferred to polyvinylidene difluoride membranes. Membranes were incubated overnight in primary antibody, washed, and incubated with horseradish peroxidase-conjugated goat anti-mouse IgG (MP Biomedicals, Irvine, CA, USA) for 1 h. Enhanced chemiluminescence (ECL) substrate (Amersham Biosciences, Piscataway, NJ, USA) was added before exposure to X-ray film. Blots were quantified using Multigauge (Fujifilm, Stamford, CT, USA) and the density of signal was normalized to 2N littermate signal levels. Data were presented as the ratio of Ts65Dn band intensity to that of 2N littermate (mean ± SEM). Uniformity of loading was confirmed by Ponceau S staining, β-actin, and β-tubulin probing.

Soluble proteins were extracted from hemibrain homogenates using 0.2% diethylamine followed by centrifugation at 135 000 *g* for 1 h (Schmidt *et al.* 2005a). To differentiate sAPPα and sAPPβ, the soluble protein extract containing both sAPP species was immunoprecipitated overnight using m3.2 (2 μg/μL) to isolate murine sAPPα. Equivalent amounts of immunoprecipitate and supernatant were electrophoresed, transferred to membrane, and probed with 22C11.

Aβ was measured as previously described following diethylamine extraction (Schmidt *et al.* 2005a). Sandwich ELISAs to detect murine Aβ40 or Aβ42 were carried out as previously reported with

m3.2 antibody used for detection (Schmidt *et al.* 2005a). ELISA plates were developed using a color reaction (TMB Microwell Peroxidase Substrate System; Kirkegaard & Perry Laboratories, Gaithersburg, MD, USA) and read against synthetic murine Aβ standards of known concentration.

mRNA analysis

App mRNA levels were analyzed by qPCR as previously described (Ginsberg 2005; Ginsberg and Mirnics 2006; Ginsberg *et al.* 2006; Alldred *et al.* 2009). qPCR was performed using Taqman PCR primers (Applied Biosystems, Foster City, CA, USA) for the murine *App* gene (ABI Assay Mm00431827_m1), *SOD1* gene (ABI Assay Mm01344232_g1), *DYRK1A* (ABI Assay Mm00432934_m1), and the housekeeping gene *GAPDH* (ABI Assay Mm99999915_G1) as a control. Samples were run on a real-time PCR cycler (7900HT; Applied Biosystems) as per the manufacturer's instructions. Standard curves and cycle threshold were measured using standards obtained from brain RNA. The ddCT method was employed to determine relative gene level differences. A total of three to four independent samples per subject were assayed in triplicate.

Statistical analysis

SPSS (Chicago, IL, USA) was used to conduct one-way ANOVAs for all analyses with *post hoc* analysis (Neumann–Keuls test; level of statistical significance was set at 0.05) for individual comparisons. Error bars were SEM.

Results

App message levels remain at diploid levels in Ts65Dn mouse brain at 5 months of age

Hemibrains lacking cerebellum from 5-month-old ($n = 4$ Ts65Dn, $n = 4$ 2N) and 12-month-old ($n = 4$ Ts65Dn, $n = 4$ 2N) Ts65Dn mice and 2N littermate controls were analyzed via real-time qPCR using a Taqman assay (Ginsberg 2005; Ginsberg and Mirnics 2006; Ginsberg *et al.* 2006). *App* message levels in the aged 12-month-old Ts65Dn mice were 1.80 ± 0.21-fold higher ($p < 0.005$) than in 2N littermate controls while 5-month-old Ts65Dn mice had similar levels (0.92 ± 0.06-fold) to 2N controls (Fig. 1),

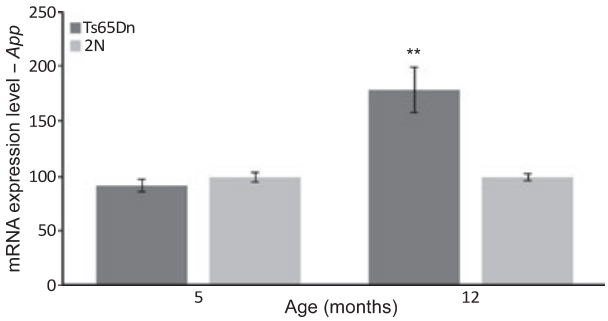

Fig. 1 Brain *App* mRNA levels in Ts65Dn mouse increase with age. Relative expression levels of *App* in Ts65Dn mouse brain were found by real-time qPCR and are shown in this histogram, with error bars representing SEM. The double asterisk (**) indicates a significant increase ($p < 0.005$) in *App* expression in the 12-month-old Ts65Dn mouse brain compared with 12-month-old 2N littermates as well as 5-month-old Ts65Dn and 2N mice.

in close agreement with our western blot data on APP holoprotein levels.

APP holoprotein levels in the Ts65Dn brain increase with age

Levels of APP in 4-month-old trisomic mice were similar to levels in 2N mice (1.1 ± 0.03-fold of 2N, $n = 5$ Ts65Dn, $n = 5$ 2N) (Fig. 2a, lanes 2–7). Given the increased *App* gene dosage in these mice, it was unexpected that APP levels did not track with gene copy number in the 4-month-old trisomic mice. In contrast, a 1.8 ± 0.08-fold ($p < 0.005$; $n = 9$ Ts65Dn, $n = 11$ 2N) increase in endogenous APP levels was seen in 12-month-old Ts65Dn mice compared with 12-month-old 2N mice (Fig. 2a, lanes 8–13). We next examined APP levels in Ts65Dn mice at 2-month intervals between 2 and 12 months of age, and a representative western blot is shown in Fig. 2b. APP levels did not change as a function of age in control 2N mice. APP levels in hemibrain homogenates were similar in Ts65Dn mice up to 8 months of age when compared with 2N mice (2-month-old: Ts65Dn levels: 1.1-fold of 2N, $n = 1$ Ts65Dn, $n = 1$ 2N; 6-month-old: Ts65Dn levels: 1.1 ± 0.13-fold of 2N, $n = 2$ Ts65Dn, $n = 3$

Fig. 2 Brain APP holoprotein levels in Ts65Dn mouse increase with age. (a) Hemibrains lacking cerebellum of Ts65Dn (Ts) mice and diploid littermate controls (2N) were isolated, homogenized, and western blots were probed with an anti-APP C-terminal monoclonal antibody (C1/6.1) (Mathews *et al.* 2002). Representative immunoblots showed differences in APP holoprotein levels as Ts65Dn mice age. (b) APP holoprotein levels are shown in Ts65Dn and 2N littermates at the indicated ages in a representative western blot. The blot was stripped and reprobed with anti β-actin antibody as a loading control (lower panel). Quantitation is depicted in histogram to the right with error bars representing SEM. The double asterisk (**, $p < 0.005$) and the single asterisk (*, $p < 0.05$) indicate a significant increase. (c) Hippocampus (lanes 1–4), cingulate cortex (lanes 5–8), striatum (lanes 9–12), and temporal cortex (lanes 13–16) from 12-month-old mice of the indicated genotypes were regionally dissected, homogenized, and subjected to immunoblot analysis using C1/6.1. Quantitation is depicted in histogram to the right with error bars representing SEM. (d) SOD1 levels are shown in Ts65Dn and 2N littermates at the indicated ages in a representative western blot. The blot was stripped and reprobed with anti-β-tubulin antibody as a loading control (lower panel). (e,f) Relative expression levels of *SOD1* (e) and *DYRK1A* (f) in Ts65Dn mouse brain were determined by real-time qPCR and are shown in the histogram, with error bars representing SEM. The single asterisks indicate a significant increase ($p < 0.05$) in gene expression in the 12-month-old Ts65Dn mouse brain compared with 12-month-old 2N littermates as well as 5-month-old Ts65Dn and 2N mice.

2N; 8-month-old: Ts65Dn levels: 1.0 ± 0.08-fold of 2N, $n = 2$ Ts65Dn, $n = 3$ 2N), yet APP levels differed significantly in 10-month-old (Ts65Dn levels: 1.5 ± 0.17-fold of 2N, $n = 3$ Ts65Dn, $n = 1$ 2N, $p < 0.05$) as well as the 12-month-old Ts65Dn mice when compared with 2N levels. Across multiple brain regions, APP levels were increased in 12-month-old Ts65Dn mice, with hippocampus (1.8 ± 0.16-fold of 2N, lanes 1–4) and temporal cortex (1.6 ± 0.08-fold

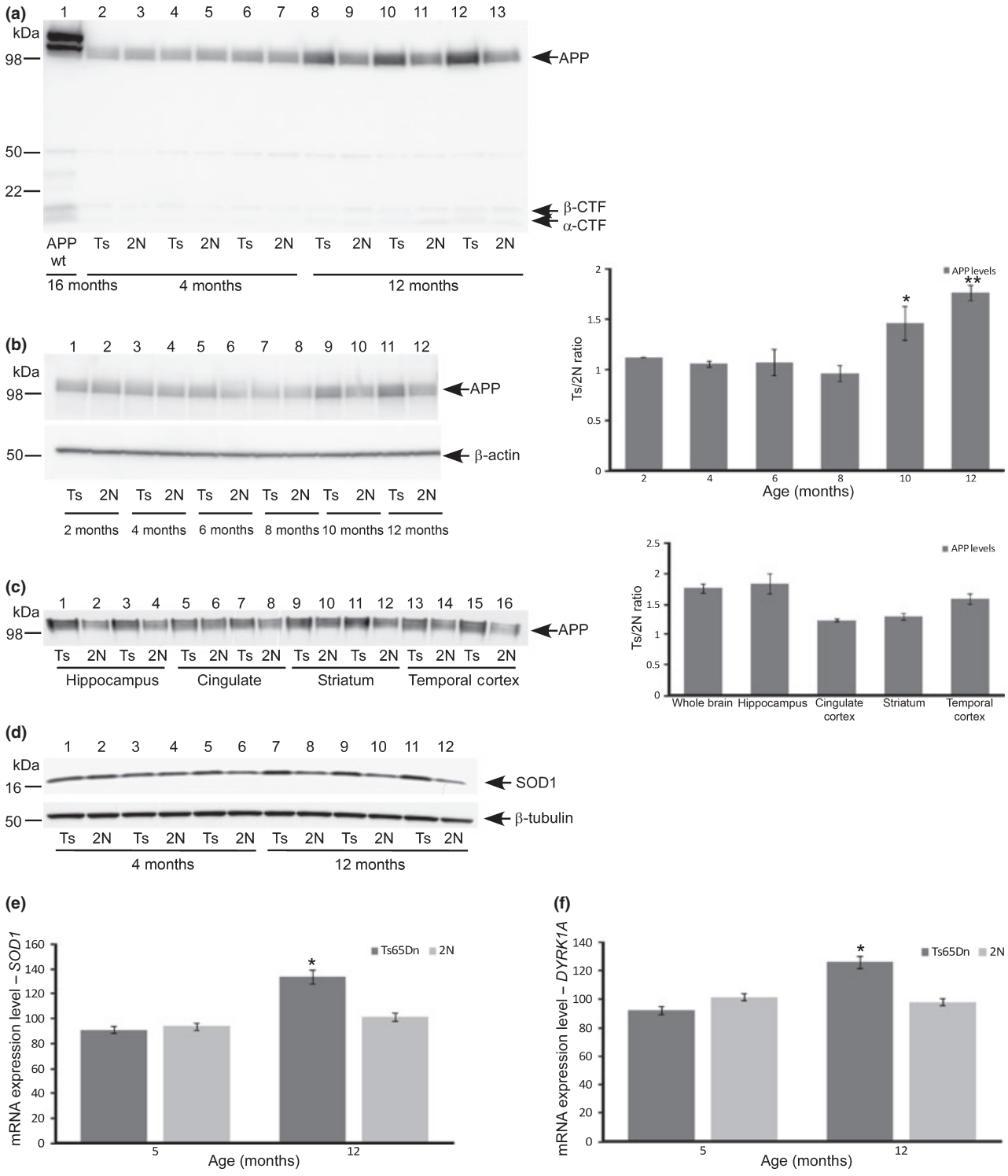

of 2N, lanes 13–16) showing the greatest increase, and cingulate cortex (1.2 ± 0.02-fold of 2N, lanes 5–8) and striatum (1.3 ± 0.06-fold of 2N, lanes 9–12) showing a lesser increase (Fig. 2c).

In addition to APP, we examined the brain expression with aging of two additional genes, *SOD1* and *DYRK1A*, that were also triplicated in the Ts65Dn mouse as well as triplicated in human DS. Similar to APP, SOD1 protein levels were not elevated in hemibrain homogenates of 4-month-old Ts65Dn mice when compared with 2N mice (Fig. 2d; 1.1 ± 0.37-fold of 2N, $n = 3$ Ts65Dn, $n = 3$ 2N) but was elevated in 12-month-old Ts65Dn mice (1.7 ± 0.24-fold of 2N, $n = 3$ Ts65Dn, $n = 3$ 2N, $p < 0.01$). qPCR analysis of 12-month-old Ts65Dn mouse hemibrains showed a 1.34 ± 0.06-fold increase in *SOD1* message levels ($p < 0.05$) compared with 2N littermate controls while 5-month-old Ts65Dn mice had similar levels (0.91 ± 0.03-fold) compared with 2N controls (Fig. 2e), in agreement with our SOD1 protein western blot data. A similar finding for *DYRK1A* mRNA was seen (Fig. 2f) with increased message levels in 12-month-old Ts65Dn mice (1.26 ± 0.13-fold, $p < 0.05$) when compared with age-matched littermate 2N controls and younger 5-month-old Ts65Dn and 2N mice (0.92 ± 0.08-fold).

APP metabolite levels in the Ts65Dn brain

We next compared the levels of sAPP in the brains of Ts65Dn mice to 2N littermate controls. Soluble proteins were examined by western blot analysis using 22C11 which detects both α- and β-cleaved sAPP species (Fig. 3a). In agreement with the levels of APP holoprotein (Fig. 2a and b), the levels of total sAPP were found to be similar between Ts65Dn and 2N mice at 4 months of age (Ts65Dn 1.0 ± 0.10-fold of 2N, $n = 3$ Ts65Dn, $n = 3$ 2N). At 12 months of age, sAPP levels were increased (1.3 ± 0.06-fold, $n = 3$ Ts65Dn, $n = 3$ 2N) in the Ts65Dn compared with 2N mice. The specificity of the 22C11 signal for sAPP was demonstrated by the lack of any reactivity in an APP null mouse (Fig. 3a, lane 13).

To determine whether the levels of sAPPα or sAPPβ were both similarly increased, or whether α- or β-cleavage was specifically altered in the Ts65Dn mice, a soluble protein extract containing both sAPP species was immunoprecipitated using the monoclonal antibody m3.2 to isolate sAPPα. This immunoprecipitation procedure, which fully recovered murine sAPPα (data not shown), was resolved along with an equal quantity of the sAPPβ-containing supernatant of the immunoprecipitation and sAPP species detected using 22C11 (Fig. 3b and c). In 4-month-old mice (Fig. 3b), the levels of both sAPPα and sAPPβ were found to be similar between Ts65Dn and 2N mice (sAPPα: Ts65Dn 1.0 ± 0.09-fold of 2N, $n = 3$ Ts65Dn, $n = 3$ 2N; sAPPβ: Ts65Dn 1.0 ± 0.07-fold 2N, $n = 3$ Ts65Dn, $n = 3$ 2N). In 12-month-old mice (Fig. 3c), however, the levels of both sAPPα and sAPPβ were increased in the Ts65Dn brain relative to 2N mice (sAPPα: Ts65Dn 1.3 ± 0.18-fold of 2N, $n = 3$ Ts65Dn, $n = 3$ 2N; sAPPβ: Ts65Dn 1.4 ± 0.07-fold 2N, $n = 3$ Ts65Dn, $n = 3$ 2N). Thus, brain levels of both sAPPα and sAPPβ were increased in 12-month-old Ts65Dn mice, commensurate with increased brain levels of total sAPP in 12-month-old Ts65Dn mice. While the increase in APP holoprotein, total sAPP, and the β-cleaved sAPPβ in aged Ts65Dn mice predicted a similar increase in brain Aβ levels, unexpectedly no significant increase was seen in the Ts65Dn mouse brain compared with 2N tissue for CTFs (4-month-old αCTF: Ts65Dn 1.27 ± 0.09-fold of 2N, $n = 3$ Ts65Dn, $n = 3$ 2N; 4-month-old βCTF: Ts65Dn 1.36 ± 0.22-fold 2N, $n = 3$ Ts65Dn, $n = 3$ 2N; 12-month-old αCTF: Ts65Dn 1.21 ± 0.35-fold of 2N, $n = 3$ Ts65Dn, $n = 3$ 2N; 12-month-old βCTF: Ts65Dn 0.93 ± 0.24-fold 2N, $n = 3$ Ts65Dn, $n = 3$ 2N; Fig. 3d), Aβ40 (Fig. 3e upper panel), and Aβ42 (Fig. 3e lower panel) at ages examined. The lack of an increase in brain Aβ levels, given the increase in APP, total sAPP, and the β-cleaved sAPPβ in aged Ts65Dn led us to examine the levels of two important Aβ degrading enzymes, IDE, and neprilysin (Fig. 3f). There were no significant differences in IDE or neprilysin levels in the Ts65Dn mouse brain compared with 2N at 4 or 12 months of age.

Turnover of APP metabolites in the Ts65Dn brain

Although the age-dependent increase of brain APP levels in Ts65Dn was explained by gene dosage-driven changes in APP biosynthesis, the subsequent lack of increase in brain Aβ levels in Ts65Dn led us to examine the turnover of APP metabolites in the Ts65Dn mouse brain. To examine APP turnover in the intact brain, 12-month-old Ts65Dn and 2N littermate mice were injected with the protein synthesis inhibitor cycloheximide to block *de novo* synthesis of APP. APP had a short half-life in cultured neurons (LeBlanc *et al.* 1996) and it was substantially degraded within a few hours in the murine brain (Morales-Corraliza J., Mazzella M.J., Berger J.D., Diaz N.S., Choi J.H.K., Levy E., Matsuoka Y., Planel E. and Mathews P.M., unpublished data). Figure 4a shows a western blot analysis of brain APP levels following protein synthesis inhibition. In agreement with the findings shown in Fig. 2a, the initial levels of APP were greater in the Ts65Dn mice than in the 2N mice (compare lane 8 with lane 1 of Fig. 4a). The rate of decline in the level of APP in the brain following cycloheximide treatment was found to be similar between 12-month-old Ts65Dn mice and their 2N littermates, although potentially more rapid in the Ts65Dn mouse brain ($t_{½}$ ∼1.5–2 h) compared with 2N mouse brain ($t_{½}$ ∼2 h).

In addition, we examined the levels of CTFs following cycloheximide treatment (Fig. 4b). Although brain levels of both APP and sAPP were increased in the Ts65Dn mouse brain, CTF levels were not significantly increased in the Ts65Dn mouse brain at 12 months of age (12-month-old αCTF: Ts65Dn 1.2 ± 0.20-fold of 2N, $n = 3$ Ts65Dn, $n = 3$

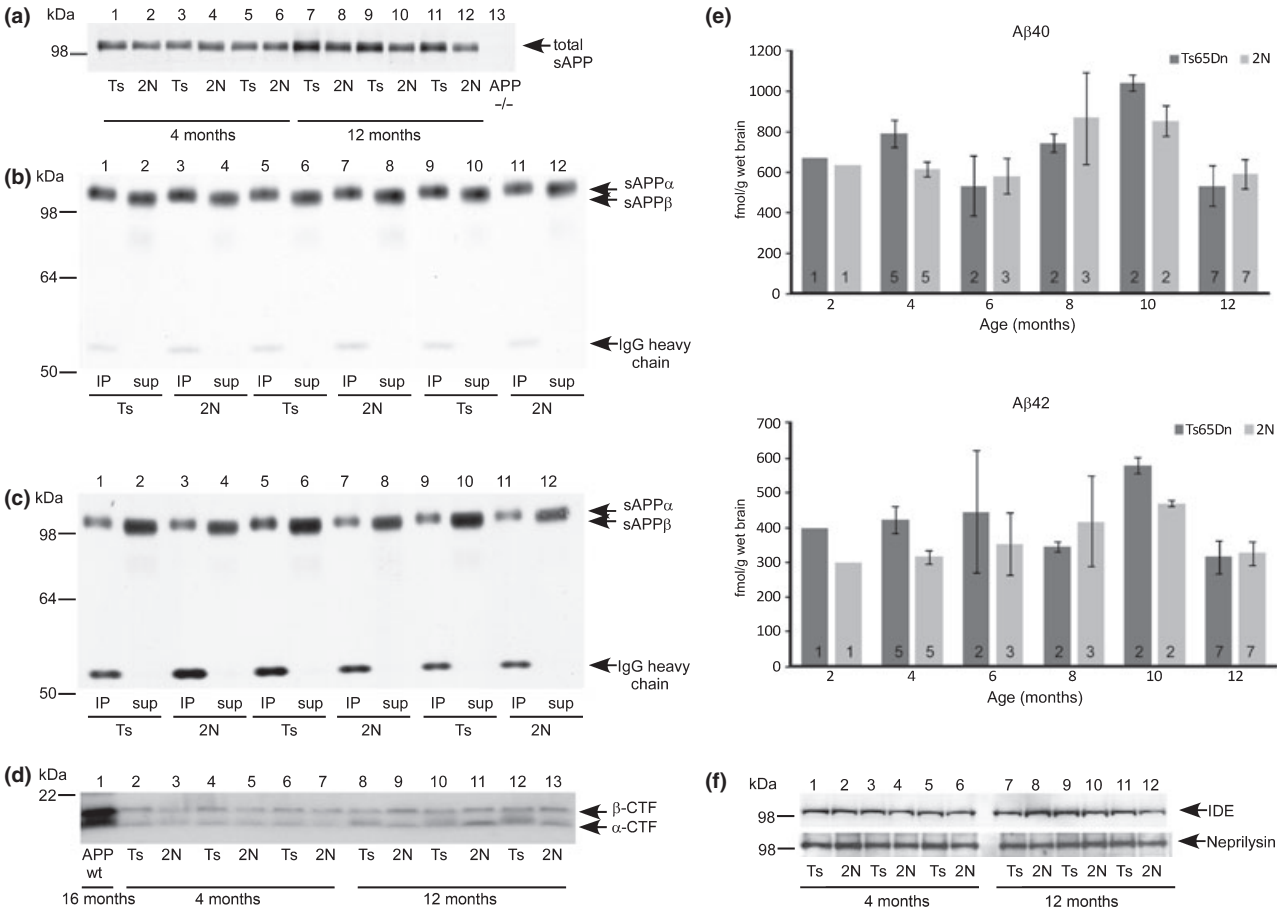

Fig. 3 APP metabolite levels and Aβ degrading enzyme levels in Ts65Dn mouse brain. (a) Soluble brain proteins were isolated as described in Materials and methods and total sAPP levels were determined by immunoblot analysis using 22C11. Ages and genotypes are as indicated. An APP null mouse (lane 13) is shown to demonstrate the specificity of the sAPP signal. **(**b,c**)** Soluble brain proteins were immunoprecipitated with m3.2 monoclonal antibody to immunoisolate sAPPα, and equivalent amounts of immunoprecipitate and supernatant were migrated, transferred to membrane, and probed with 22C11. Levels of endogenous sAPPα and sAPPβ in 4-month-old (b) and 12-month-old (c) mice are shown. (d) APP C-terminal fragments (CTFs) were detected by western blot analysis using C1/6.1. Hemibrain homogenates from 4-month-old (lanes 2–7) and 12-month-old (lanes 8–13) Ts65Dn mouse brain and their littermate controls are shown. APPwt is shown in lane 1 as a positive control. (e) Levels of Aβ40 and Aβ42 were quantitated by sandwich ELISA. Ages and genotypes are as indicated. Sample sizes are as indicated within the histograms with error bars representing SEM. (f) Hemibrain lacking cerebellum homogenates of indicated ages and genotypes were probed for Aβ degrading enzymes IDE (upper panel) and neprilysin (lower panel) using antibodies IDE1 and CD10 (clone 56C6) respectively.

2N; 12-month-old βCTF: Ts65Dn 0.9 ± 0.14-fold 2N, $n = 3$ Ts65Dn, $n = 3$ 2N; compare lane 8 with lane 1 of Figs. 4b and 3d). Following cycloheximide treatment, the rate of clearance of CTFs in the 12-month-old Ts65Dn mouse brain was similar to that of the 2N littermates.

We also examined the clearance rate of total sAPP (Fig. 4c). As sAPP is more stable than APP (Morales-Corraliza J., Mazzella M.J., Berger J.D., Diaz N.S., Choi J.H.K., Levy E., Matsuoka Y., Planel E. and Mathews P.M., unpublished data), we extended the time-course of cycloheximide treatment out to 7 h. In agreement with the findings in Fig. 3a, the initial levels of total brain sAPP in Ts65Dn were increased when compared with 2N. While 12-month-old 2N brain sAPP levels were found to be highly stable over the 7-hour period of cycloheximide treatment, the 12-month-old Ts65Dn brain sAPP turnover was more rapid ($t_{½}$ ~7 h). Finally, the clearance of brain Aβ40 and Aβ42 was examined in the 12-month-old Ts65Dn mouse following cycloheximide treatment (Fig. 4d). The turnover rates were similar in the Ts65Dn mouse compared with 2N, although this methodology might exaggerate the half-life of Aβ in the brain because of the continued presence of APP during the initial time-points following the inhibition of protein synthesis.

Discussion

Although copy number-dependent over-expression of triplicated genes on the HSA21 locus in DS was observed

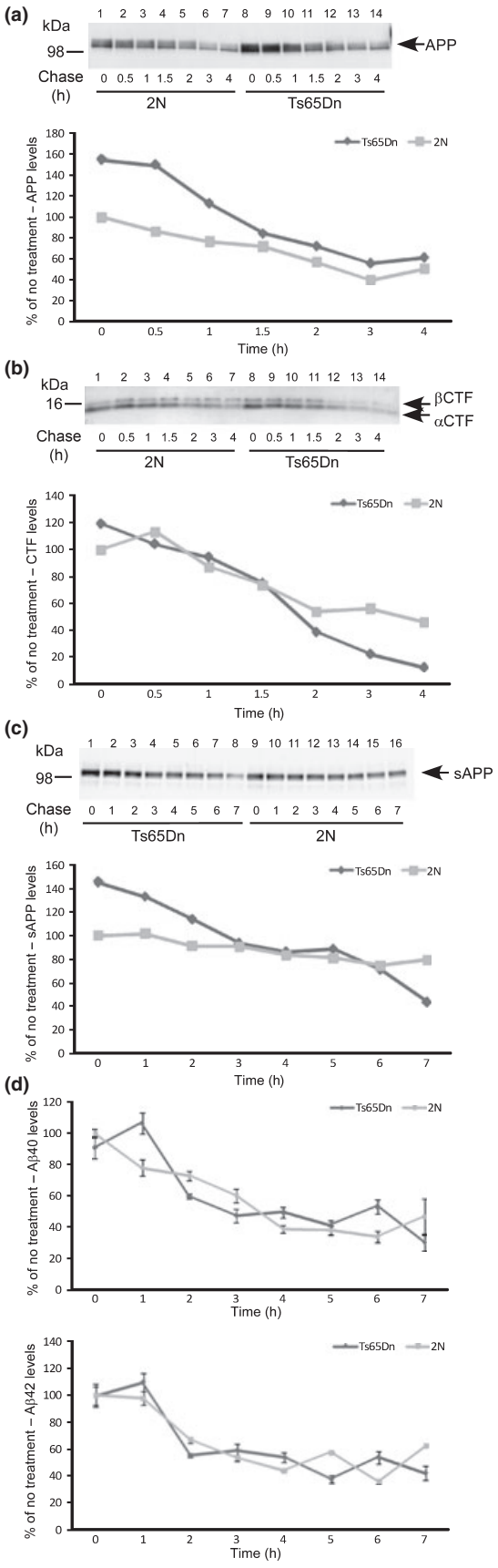

Fig. 4 APP metabolite turnover in 12-month-old Ts65Dn mouse brain. APP metabolite turnover was followed after treatment of 12-month-old 2N and Ts65Dn mice with the protein synthesis inhibitor cycloheximide (100 μL of 150 μg/mL). Brain APP holoprotein levels (a) and CTF levels (b) were determined at the indicated times following cycloheximide treatment by western blot analysis of hemibrain lacking cerebellum homogenates using C1/6.1. The corresponding quantitation as a percentage of control (2N mouse brain at time 0 of cycloheximide treatment) is shown by the graphics below the western blots. (c**)** Total sAPP turnover following cycloheximide treatment was determined via immunoblot analysis of diethylamine-extracted soluble proteins using 22C11. Quantitation is shown below. (d**)** Aβ40 and Aβ42 turnover following cycloheximide treatment was quantitated by sandwich ELISA. Error bars represent SEM.

(FitzPatrick *et al.* 2002), not all trisomic genes were overexpressed, and there was substantial variation in the increase in individual triplicated genes (Mao *et al.* 2005; Lockstone *et al.* 2007). Similarly, the Ts65Dn model of DS showed an increase in transcript levels of triplicated genes across multiple tissues (Saran *et al.* 2003; Kahlem *et al.* 2004). Nevertheless, there was variation of gene expression in the Ts65Dn mice, with many of the genes in dosage imbalance not expressing at the expected 1.5-fold increase in the brain at various ages (Lyle *et al.* 2004; Sultan *et al.* 2007). For example, our findings with *DYRK1A* were consistent with those published by Sultan *et al.* (2007), which showed no increase in *DYRK1A* mRNA levels in 4-month-old Ts65Dn mice, although older mice were not examined. In human DS, while APP protein (Rumble *et al.* 1989) and *App* mRNA levels (Oyama *et al.* 1994) appeared to be increased in aged brain, other studies have shown limited changes in *App* message when DS individuals were compared with diploid (Lockstone *et al.* 2007) and contradictory findings have been reported from fetal tissue (Argellati *et al.* 2006). APP (Salehi *et al.* 2006) and combined APP/sAPP (Hunter *et al.* 2003a; Seo and Isacson 2005) protein levels have been shown to be increased in the brains of 12-month-old and older Ts65Dn mice. In addition, Hunter *et al.* (2003b) have shown an age-dependent increase in the combined APP/sAPP protein expression they detected in the Ts65Dn mouse brain, with changes apparent at an earlier age in the striatum and later in the cortex. At 12 months of age, we have shown that this increased signal in the brain consists not only of the parental APP protein but also the two sAPP species. The reported findings on *App* mRNA levels in the Ts65Dn mouse brain were more variable, with some studies suggesting an increase in *App* mRNA in both young and old Ts65Dn mice (Lyle *et al.* 2004), while others have suggested that some brain regions show an increase in *App* mRNA in young Ts65Dn mouse brain (Sultan *et al.* 2007). Our findings suggest that age-dependent changes occur in the expression of multiple triplicated genes in the Ts65Dn brain, both at the level of the mRNA (*App, SOD1, DYRK1A*) and at the level of the protein (APP, SOD1).

Age-dependent increase in brain APP protein levels is intriguing given that BFCN degeneration in the Ts65Dn mouse is also age-dependent, initially detected at ~6 months of age (Holtzman *et al.* 1996; Granholm *et al.* 2000) with continued phenotypic loss of cholinergic neurons through 12 months of age (Cooper *et al.* 2001). The loss of this group of neurons has been correlated with decreasing spatial memory in 6-month-old Ts65Dn mice compared with 4-month-old Ts65Dn mice. Thus, while the Ts65Dn mouse has limited behavioral deficits at 4 months of age, these deficits increase in severity with aging (Hunter *et al.* 2003a), a phenotypic worsening that may drive or be driven by the apparent age-dependent dysregulation of various triplicated gene transcripts, including *App*. Additionally, multiple lines of evidence have argued that BFCNs are particularly vulnerable to insults linked at some level to APP metabolite dysregulation in the brain. In AD, loss of BFCNs is a prominent feature of the disease (Whitehouse *et al.* 1982; Mufson *et al.* 2008). Failure of neurotrophic signaling required for BFCN maintenance and survival occurred through decrements in NGF levels, high-affinity NGF receptor-mediated endocytosis, and retrograde signaling endosome NGF trophic signaling (Delcroix *et al.* 2003; Nixon 2005; Wu *et al.* 2009). Collective dysfunction of these processes led to frank BFCN degeneration (Mufson *et al.* 1995, 1999), although how Aβ deposition or other aspects of AD pathobiology contributed to this process in AD was unclear. BFCNs in the Ts65Dn mouse showed defective retrograde transport of NGF (Cooper *et al.* 2001; Sofroniew *et al.* 2001), and exogenous addition of NGF could prevent BFCN loss (Cooper *et al.* 2001; Sofroniew *et al.* 2001). NGF retrograde transport and BFCN survival are both improved in Ts65Dn mice made diploid for the *App* gene (Salehi *et al.* 2006), demonstrating genetically that dysregulation of some aspect of APP function, likely to be dependent upon APP over-expression, contributes critically to the degeneration of this neuronal population. Similarly, *App* gene triplication is necessary for the development of neuronal endosomal pathology in the Ts65Dn mouse (Cataldo *et al.* 2003), morphological changes hypothesized to be linked to signaling endosome dysfunction and NGF trophic failure.

The present biochemical analysis of APP metabolite expression was carried out using brain homogenates that contained cortical and subcortical regions, including white matter. It is possible that APP expression is initially increased locally in a limited neuronal population, an idea that is consistent with endosomal pathology being restricted at 4 months of age to a subpopulation of medial septal neurons (Cataldo *et al.* 2003) and with increased APP levels in striatum of Ts65Dn mice 6–8 months of age (Hunter *et al.* 2003b). Indeed, *App* mRNA level increases in the Ts65Dn mouse brain coincided broadly with the onset of cholinergic deficits (Holtzman *et al.* 1996; Granholm *et al.* 2000; Cooper *et al.* 2001) and increased endosomal pathology within the septohippocampal system (Cataldo *et al.* 2003). Despite an increase in *App* mRNA levels which led to increased APP holoprotein levels in aged Ts65Dn mice, our findings showed that APP and sAPP turnover was not slowed in the Ts65Dn mouse brain. Strikingly, brain Aβ levels – in spite of increased APP expression and robust β-cleavage leading to a proportionate increase in sAPPβ – remained unchanged. Greatly reducing γ-cleavage led to a stabilization of CTFs and an increase in CTF levels, which could be detected in brain (Rozmahel *et al.* 2002). We did not detect an increase in CTF levels in the aged Ts65Dn mice, nor was there an indication that the turnover of the CTFs was altered, which argued against a stabilization of CTFs as the underlying mechanism for the maintenance of brain Aβ levels in the aged Ts65Dn mouse brain. We did not detect an increased Aβ turnover rate or an increased level of two important Aβ degrading enzymes in the Ts65Dn mouse brain. Again, it is possible that critical aspects of Aβ production and turnover are altered within discrete subpopulations of neurons in the Ts65Dn mouse, and therefore not detected in a brain homogenate. Indeed it is possible, if not likely, that there are additional turnover mechanisms for APP metabolites, such as CTFs, which includes the lysosomal system, that can contribute to the turnover of CTFs without the generation of excess Aβ (Haass *et al.* 1992). While DS and triplication of small regions of HSA21 containing *App* inevitably led to AD and β-amyloid pathology (Casanova *et al.* 1985; Mann *et al.* 1989; Rovelet-Lecrux *et al.* 2006; Sleegers *et al.* 2006), presumably through a mechanism that involved increased central Aβ and its accumulation over time, triplication of murine *App* does not lead to β-amyloid plaque pathology in the Ts65Dn mouse model. This may reflect that the more aggregative prone human Aβ has a greater tendency to accumulate and stabilize in the brain parenchyma than murine Aβ, and undoubtedly also reflects the difference in life span of the two species.

Overall, our findings argue that in the Ts65Dn mouse, multiple mechanisms come into play to modulate APP and APP metabolite levels in the brain towards normal. In the young Ts65Dn mice, homeostasis of APP occurred at the level of gene transcription, with brain *App* mRNA levels identical to that of diploid in 4-month-old mice. Moreover, even in aged mice, where *App* mRNA, APP and sAPP levels approached *App* gene copy numbers, Aβ levels were maintained close to normal levels. This complex regulation of APP in a well-established trisomic mouse model of DS is consistent with an important role for APP dysregulation in the development of the neurological phenotype in the mouse, including both endocytic alterations and BFCN neurodegeneration, and emphasize the potential for neuropathological processes to occur in some circumstances as a result of APP dysregulation in the absence of increased Aβ levels or β-amyloid accumulation.

Acknowledgements

We would like to thank Dr. Marc Mercken (Janssen Pharmaceutica, Beerse, Belgium) for anti-Aβ antibodies used in the ELISAs, Dr. Dennis Selkoe (Harvard Medical School, Boston, MA, USA) for the gift of the anti-IDE antibody, Ms. Nicole S. Diaz, Mr. Tae Lee, and Mr. Stephen D. Schmidt for technical and research support, and Dr. Monika Pawlik for her maintenance of the mouse colonies. This work was supported by the NIA (AG017617 and AG029787), the NINDS (NS045205), and the Alzheimer's Association (IIRG-07-60047).

References

Alldred M. J., Che S. and Ginsberg S. D. (2009) Terminal continuation (TC) RNA amplification without second strand synthesis. *J. Neurosci. Methods* **177**, 381–385.

Argellati F., Massone S., d'Abramo C., Marinari U. M., Pronzato M. A., Domenicotti C. and Ricciarelli R. (2006) Evidence against the overexpression of APP in Down syndrome. *IUBMB Life* **58**, 103–106.

Casanova M. F., Walker L. C., Whitehouse P. J. and Price D. L. (1985) Abnormalities of the nucleus basalis in Down's syndrome. *Ann. Neurol.* **18**, 310–313.

Cataldo A. M., Petanceska S., Peterhoff C. M., Terio N. B., Epstein C. J., Villar A., Carlson E. J., Staufenbiel M. and Nixon R. A. (2003) App gene dosage modulates endosomal abnormalities of Alzheimer's disease in a segmental trisomy 16 mouse model of Down syndrome. *J. Neurosci.* **23**, 6788–6792.

Cooper J. D., Salehi A., Delcroix J. D., Howe C. L., Belichenko P. V., Chua-Couzens J., Kilbridge J. F., Carlson E. J., Epstein C. J. and Mobley W. C. (2001) Failed retrograde transport of NGF in a mouse model of Down's syndrome: reversal of cholinergic neurodegenerative phenotypes following NGF infusion. *Proc. Natl Acad. Sci. USA* **98**, 10439–10444.

Delcroix J. D., Valletta J. S., Wu C., Hunt S. J., Kowal A. S. and Mobley W. C. (2003) NGF signaling in sensory neurons: evidence that early endosomes carry NGF retrograde signals. *Neuron* **39**, 69–84.

Demas G. E., Nelson R. J., Krueger B. K. and Yarowsky P. J. (1996) Spatial memory deficits in segmental trisomic Ts65Dn mice. *Behav. Brain Res.* **82**, 85–92.

Demas G. E., Nelson R. J., Krueger B. K. and Yarowsky P. J. (1998) Impaired spatial working and reference memory in segmental trisomy (Ts65Dn) mice. *Behav. Brain Res.* **90**, 199–201.

FitzPatrick D. R., Ramsay J., McGill N. I., Shade M., Carothers A. D. and Hastie N. D. (2002) Transcriptome analysis of human autosomal trisomy. *Hum. Mol. Genet.* **11**, 3249–3256.

Ginsberg S. D. (2005) RNA amplification strategies for small sample populations. *Methods* **37**, 229–237.

Ginsberg S. D. and Mirnics K. (2006) Functional genomic methodologies. *Prog. Brain Res.* **158**, 15–40.

Ginsberg S. D., Che S., Wuu J., Counts S. E. and Mufson E. J. (2006) Down regulation of trk but not p75NTR gene expression in single cholinergic basal forebrain neurons mark the progression of Alzheimer's disease. *J. Neurochem.* **97**, 475–487.

Gold P. E. and Sternberg D. B. (1978) Retrograde amnesia produced by several treatments: evidence for a common neurobiological mechanism. *Science* **201**, 367–369.

Granholm A. C., Sanders L. A. and Crnic L. S. (2000) Loss of cholinergic phenotype in basal forebrain coincides with cognitive decline in a mouse model of Down's syndrome. *Exp. Neurol.* **161**, 647–663.

Granholm A. C., Sanders L., Seo H., Lin L., Ford K. and Isacson O. (2003) Estrogen alters amyloid precursor protein as well as dendritic and cholinergic markers in a mouse model of Down syndrome. *Hippocampus* **13**, 905–914.

Haass C., Koo E. H., Mellon A., Hung A. Y. and Selkoe D. J. (1992) Targeting of cell-surface β-amyloid precursor protein to lysosomes: alternative processing into amyloid-bearing fragments. *Nature* **357**, 500–503.

Hardy J. and Selkoe D. J. (2002) The amyloid hypothesis of Alzheimer's disease: progress and problems on the road to therapeutics. *Science* **297**, 353–356.

Holtzman D. M., Santucci D., Kilbridge J. *et al.* (1996) Developmental abnormalities and age-related neurodegeneration in a mouse model of Down syndrome. *Proc. Natl Acad. Sci. USA* **93**, 13333–13338.

Hunter C. L., Bimonte H. A. and Granholm A. C. (2003a) Behavioral comparison of 4 and 6 month-old Ts65Dn mice: age-related impairments in working and reference memory. *Behav. Brain Res.* **138**, 121–131.

Hunter C. L., Isacson O., Nelson M., Bimonte-Nelson H., Seo H., Lin L., Ford K., Kindy M. S. and Granholm A. C. (2003b) Regional alterations in amyloid precursor protein and nerve growth factor across age in a mouse model of Down's syndrome. *Neurosci. Res.* **45**, 437–445.

Kahlem P., Sultan M., Herwig R. *et al.* (2004) Transcript level alterations reflect gene dosage effects across multiple tissues in a mouse model of Down syndrome. *Genome Res.* **14**, 1258–1267.

LeBlanc A. C., Xue R. and Gambetti P. (1996) Amyloid precursor protein metabolism in primary cell cultures of neurons, astrocytes, and microglia. *J. Neurochem.* **66**, 2300–2310.

Lin X., Koelsch G., Wu S., Downs D., Dashti A. and Tang J. (2000) Human aspartic protease memapsin 2 cleaves the β-secretase site of β-amyloid precursor protein. *Proc. Natl Acad. Sci. USA* **97**, 1456–1460.

Lockstone H. E., Harris L. W., Swatton J. E., Wayland M. T., Holland A. J. and Bahn S. (2007) Gene expression profiling in the adult Down syndrome brain. *Genomics* **90**, 647–660.

Lyle R., Gehrig C., Neergaard-Henrichsen C., Deutsch S. and Antonarakis S. E. (2004) Gene expression from the aneuploid chromosome in a trisomy mouse model of Down syndrome. *Genome Res.* **14**, 1268–1274.

Mann D. M., Brown A., Prinja D., Davies C. A., Landon M., Masters C. L. and Beyreuthers K. (1989) An analysis of the morphology of senile plaques in Down's syndrome patients of different ages using immunocytochemical and lectin histochemical techniques. *Neuropathol. Appl. Neurobiol.* **15**, 317–329.

Mao R., Wang X., Spitznagel E. L. Jr, Frelin L. P., Ting J. C., Ding H., Kim J. W., Ruczinski I., Downey T. J. and Pevsner J. (2005) Primary and secondary transcriptional effects in the developing human Down syndrome brain and heart. *Genome Biol.* **6**, R107.

Mathews P. M., Jiang Y., Schmidt S. D., Grbovic O. M., Mercken M. and Nixon R. A. (2002) Calpain activity regulates the cell surface distribution of amyloid precursor protein: inhibition of calpains enhances endosomal generation of β-cleaved C-terminal APP fragments. *J. Biol. Chem.* **277**, 36415–36424.

Mufson E. J., Conner J. M. and Kordower J. H. (1995) Nerve growth factor in Alzheimer's disease: defective retrograde transport to nucleus basalis. *Neuroreport* **6**, 1063–1066.

Mufson E. J., Kroin J. S., Sendera T. J. and Sobreviela T. (1999) Distribution and retrograde transport of trophic factors in the central nervous system: functional implications for the treatment of neurodegenerative diseases. *Prog. Neurobiol.* **57**, 451–484.

Mufson E. J., Counts S. E., Perez S. E. and Ginsberg S. D. (2008) Cholinergic system during the progression of Alzheimer's disease: therapeutic implications. *Expert Rev. Neurother.* **8**, 1703–1718.

Nixon R. A. (2005) Endosome function and dysfunction in Alzheimer's disease and other neurodegenerative diseases. *Neurobiol. Aging* **26**, 373–382.

Oyama F., Cairns N. J., Shimada H., Oyama R., Titani K. and Ihara Y. (1994) Down's syndrome: up-regulation of β-amyloid protein precursor and tau mRNAs and their defective coordination. *J. Neurochem.* **62**, 1062–1066.

Qiu W. Q., Walsh D. M., Ye Z., Vekrellis K., Zhang J., Podlisny M. B., Rosner M. R., Safavi A., Hersh L. B. and Selkoe D. J. (1998) Insulin-degrading enzyme regulates extracellular levels of amyloid β-protein by degradation. *J. Biol. Chem.* **273**, 32730–32738.

Reeves R. H., Irving N. G., Moran T. H., Wohn A., Kitt C., Sisodia S. S., Schmidt C., Bronson R. T. and Davisson M. T. (1995) A mouse model for Down syndrome exhibits learning and behaviour deficits. *Nat. Genet.* **11**, 177–184.

Rovelet-Lecrux A., Hannequin D., Raux G. *et al.* (2006) APP locus duplication causes autosomal dominant early-onset Alzheimer disease with cerebral amyloid angiopathy. *Nat. Genet.* **38**, 24–26.

Rozmahel R., Huang J., Chen F. *et al.* (2002) Normal brain development in PS1 hypomorphic mice with markedly reduced γ-secretase cleavage of βAPP. *Neurobiol. Aging* **23**, 187–194.

Rumble B., Retallack R., Hilbich C., Simms G., Multhaup G., Martins R., Hockey A., Montgomery P., Beyreuther K. and Masters C. L. (1989) Amyloid A4 protein and its precursor in Down's syndrome and Alzheimer's disease. *N. Engl. J. Med.* **320**, 1446–1452.

Salehi A., Delcroix J. D., Belichenko P. V. *et al.* (2006) Increased App expression in a mouse model of Down's syndrome disrupts NGF transport and causes cholinergic neuron degeneration. *Neuron* **51**, 29–42.

Saran N. G., Pletcher M. T., Natale J. E., Cheng Y. and Reeves R. H. (2003) Global disruption of the cerebellar transcriptome in a Down syndrome mouse model. *Hum. Mol. Genet.* **12**, 2013–2019.

Schmidt S. D., Nixon R. A. and Mathews P. M. (2005a) ELISA method for measurement of amyloid-β levels. *Methods Mol. Biol.* **299**, 279–297.

Schmidt S. D., Jiang Y., Nixon R. A. and Mathews P. M. (2005b) Tissue processing prior to protein analysis and amyloid-β quantitation. *Methods Mol. Biol.* **299**, 267–278.

Seo H. and Isacson O. (2005) Abnormal APP, cholinergic and cognitive function in Ts65Dn Down's model mice. *Exp. Neurol.* **193**, 469–480.

Sleegers K., Brouwers N., Gijselinck I., Theuns J., Goossens D., Wauters J., Del-Favero J., Cruts M., van Duijn C. M. and Van Broeckhoven C. (2006) APP duplication is sufficient to cause early onset Alzheimer's dementia with cerebral amyloid angiopathy. *Brain* **129**, 2977–2983.

Sofroniew M. V., Howe C. L. and Mobley W. C. (2001) Nerve growth factor signaling, neuroprotection, and neural repair. *Annu. Rev. Neurosci.* **24**, 1217–1281.

Sultan M., Piccini I., Balzereit D., Herwig R., Saran N. G., Lehrach H., Reeves R. H. and Yaspo M. L. (2007) Gene expression variation in Down's syndrome mice allows prioritization of candidate genes. *Genome Biol.* **8**, R91.

Vetrivel K. S. and Thinakaran G. (2006) Amyloidogenic processing of β-amyloid precursor protein in intracellular compartments. *Neurology* **66**, S69–S73.

Wallace W. C., Akar C. A. and Lyons W. E. (1997) Amyloid precursor protein potentiates the neurotrophic activity of NGF. *Brain Res. Mol. Brain Res.* **52**, 201–212.

Wang C., Wurtman R. J. and Lee R. K. (2000) Amyloid precursor protein and membrane phospholipids in primary cortical neurons increase with development, or after exposure to nerve growth factor or Aβ(1–40). *Brain Res.* **865**, 157–167.

Whitehouse P. J., Price D. L., Struble R. G., Clark A. W., Coyle J. T. and Delon M. R. (1982) Alzheimer's disease and senile dementia: loss of neurons in the basal forebrain. *Science* **215**, 1237–1239.

Wu C., Cui B., He L., Chen L. and Mobley W. C. (2009) The coming of age of axonal neurotrophin signaling endosomes. *J. Proteomics* **72**, 46–55.

